Artemether inhibits proliferation, invasion and migration of hepatocellular carcinoma cells via targeting of CYP2J2

XIONGLIN ZHU[1*], MEI YANG[2*], ZHILING SONG[1], GUANGBING YAO[1] and QIFENG SHI[3]

[1]Department of Infectious Disease, People's Hospital of Xinzhou District; [2]Department of Obstetrics and Gynecology, Xinzhou District Maternity and Child Health Hospital; [3]Department of Thoracic Surgery, Xinzhou District People's Hospital, Wuhan, Hubei 431400, P.R. China

Received September 16, 2021; Accepted January 25, 2022

DOI: 10.3892/ol.2022.13300

Abstract. Artemether, a natural derivative of artemisinin, serves an antitumor role in numerous types of cancer. However, the role and mechanism of action of artemether in hepatocellular carcinoma (HCC) has remained elusive. The present study aimed to investigate whether artemether is able to inhibit the proliferation, invasion and migration of HCC cells by targeting cytochrome P450 family 2 subfamily J member 2 (CYP2J2). Cell Counting Kit-8 (CCK-8) and colony-formation assays were used to examine cell viability. Wound-healing and Transwell assays were used to evaluate the cell invasion and migration ability. The expression levels of the epithelial-mesenchymal transition-related proteins E-cadherin, N-cadherin and vimentin were detected via western blot analysis. To determine the mechanism of the inhibitory effect of artemether on HCC, CYP2J2 was overexpressed and its expression in cells treated with artemether was confirmed using reverse transcription-quantitative PCR and western blot analysis. The effects of artemether on the viability, proliferation and migration of HCC cells overexpressing CYP2J2 were detected using CCK-8, colony-formation, wound-healing and Transwell assays, respectively. Artemether was demonstrated to exert a significant inhibitory effect on the proliferation, invasion and migration of HCC cells. Furthermore, artemether also inhibited CYP2J2 expression in Hep3B2.1-7 cells and CYP2J2 overexpression reversed the inhibitory effect of artemether on the proliferation, invasion and migration of HCC cells. Overall, these results indicated that artemether may inhibit HCC cell proliferation, invasion and migration via targeting CYP2J2. These findings may provide potential targets for future HCC therapeutics.

Correspondence to: Dr Qifeng Shi, Department of Thoracic Surgery, Xinzhou District People's Hospital, 61 Xinzhou Street, Xinzhou, Wuhan, Hubei 431400, P.R. China
E-mail: shiqifeng3370@163.com

*Contributed equally

Key words: artemether, hepatocellular carcinoma, cytochrome P450 family 2 subfamily J member 2, proliferation, invasion, migration

Introduction

Artemether, a derivative of artemisinin, is widely used as an antimalarial drug (1-3), including in cerebral malaria (4), which is caused by the parasite *Plasmodium falciparum* (5). Increasing evidence indicates that artemether also has significant antineoplastic effects. A recent study by Chen *et al* (6) reported that artemether alleviates the progression of non-small cell lung cancer by inducing apoptosis and cell cycle arrest and promoting cell senescence. Wu *et al* (7) demonstrated that the heat shock protein 90/Akt signaling pathway mediates artemether-induced apoptosis of Cal27 cells in tongue squamous cell carcinoma. Another study indicated that artemether inhibits proliferation and induces apoptosis in diffuse large B-cell lymphoma (8). However, the mechanism of action of artemether in hepatocellular carcinoma (HCC) has remained to be fully elucidated. Therefore, the present study aimed to evaluate the antitumor effect and mechanism of action of artemether in HCC.

The cytochrome P450 (CYP450) cyclooxygenases are a subgroup of heme-containing enzymes capable of epoxidation of polyunsaturated fatty acids and the metabolism of exogenous drugs. These enzymes therefore serve an important role in metabolism and organ-specific toxicity. Studies have indicated that CYP family 2 subfamily J member 2 (CYP2J2) is not only expressed in the heart, but also in the liver, kidney and lung (9-12). The expression of human CYP enzyme in human placenta, fetal liver and adult liver was characterized from macroscopic and microscopic perspectives. Compared with fetal tissue, CYPs were mainly expressed in the adult liver (9). Bièche *et al* (13) analyzed the mRNA levels of each CYP subtype in total RNA from human organ specimens and also proved that CYP2J2 is expressed in liver tissue. In recent years, CYP2J2 has been demonstrated to be upregulated in a variety of tumor types and has therefore attracted increasing attention (11,14). By analyzing CYP2J2 mRNA and protein expression levels, researchers have indicated that, compared with healthy human cell lines or tissues, CYP2J2 expression levels are increased in human-derived cancer cell lines and human cancer tissues, indicating that CYP2J2 is a positive

regulator of cancer-cell proliferation (15). A previous study demonstrated that CYP2J2 gene knockdown is able to inhibit the release of 11,12-epoxyeicosatrienoic acid, thereby inhibiting the angiogenic function of M2 microglia and significantly enhancing the antitumor effect of the cannabinoid receptor 2 agonist JWH133 on glioma (16). Furthermore, it has been demonstrated that 6,8-diphenylpropylene glycol induces apoptosis of human HCC cells by activating forkhead box O3 and inhibiting CYP2J2 (10). Gui *et al* (17) reported that increased expression of CYP2J2 in HCC cells upregulated the expression of 14,15-epoxyeicosatrienoic acid, which improved the stability of hypoxia-inducible factor-1α and finally promoted the malignant development of HCC. Therefore, CYP2J2 has the potential to be a therapeutic target for HCC.

According to the STITCH database (http://stitch.embl.de/), artemether may target CYP2J2. It may therefore be hypothesized that artemether is able to inhibit the malignant process of HCC via targeting of CYP2J2. In the present study, the effects of artemether and CYP2J2 on the proliferation, invasion and migration of HCC cells and the underlying mechanisms were investigated, in the hope that the results will provide a basis for the understanding of the antitumor effects of artemether and indicate a novel target and strategy for the clinical treatment of patients with HCC.

Materials and methods

Cell culture. The human HCC cell line Hep3B2.1-7 and the human embryonic hepatocyte cell line HHL-5 were obtained from The Cell Bank of Type Culture Collection of The Chinese Academy of Sciences. The cells were cultured in DMEM (Gibco; Thermo Fisher Scientific, Inc.) supplemented with 10% FBS (Gibco; Thermo Fisher Scientific, Inc.), 100 U/ml penicillin and 100 μg/ml streptomycin (Invitrogen; Thermo Fisher Scientific, Inc.) at 37˚C in a humidified atmosphere with 5% CO_2.

Bioinformatics analysis. The STITCH database (version 5.0; http://stitch.embl.de/) is a database that may be used to predict interactions between artemether and CYP2J2 (confidence, 0.400). In the STITCH database, each protein-protein interaction is annotated with one or more 'scores'. Of note, these scores do not indicate the strength or the specificity of the interaction. Instead, they are indicators of confidence, i.e. how likely STITCH judges an interaction to be true, given the available evidence. The minimum required interaction score is divided into the following categories: Highest confidence (0.900); high confidence (0.700); intermediate confidence (0.400) and low confidence (0.150). The ENCORI website (https://starbase.sysu.edu.cn/panGeneDiffExp.php) is used to predict CYP2J2 expression in HCC and noncancerous liver cells. The expression data of cancers were downloaded from The Cancer Genome Atlas project via the Genomic Data Commons Data Portal (https://gdc.cancer.gov). The expression values of genes from RNA-sequencing data were scaled as log2(FPKM + 0.01).

Cell Counting Kit-8 (CCK-8) assay. The CCK-8 assay was performed to assess cell viability. In brief, cells were inoculated in 96-well plates at a density of $8x10^3$ cells/well, with different concentrations (20, 40, 80 and 160 μM) of artemether (Chemical Abstracts Service no. 71963-77-4; Toronto Research Chemicals) and incubated at 37˚C for 24, 48 and 72 h, control without artemether. Following incubation, 10 μl CCK-8 reagent was added into each well and cells were cultured for another 2 h at 37˚C. The absorbance in each well was measured at a wavelength of 450 nm using a microplate reader (BioTek Instruments, Inc.).

Colony-formation assay. Hep3B2.1-7 cells ($1x10^3$ cells/well) were suspended in DMEM supplemented with 10% FBS and were seeded into 6-well plates and cultured in a 5% CO_2 incubator at 37˚C for 14 days with different concentrations (20, 40 and 80 μM) of artemether, while cells without artemether were used as a control. Subsequently, the cells were fixed using 4% paraformaldehyde at room temperature for 20 min and stained with 0.05% crystal violet solution for 25 min at 37˚C. Finally, the colonies (>50 cells/colony) were counted using an Olympus BX40 light microscope (Olympus Corporation).

Wound-healing assay. Hep3B2.1-7 cells were inoculated in 6-well plates and incubated in a 5% CO_2 incubator at 37˚C until reaching 70-80% confluency. A 200-μl pipette tip was used to make linear scratches on the cell monolayer. PBS was used to wash the monolayer three times for 2 min each to remove any cell debris. Subsequently, cells were cultured with different concentrations (20, 40 and 80 μM) of artemether in an incubator containing 5% CO_2 at 37˚C and were imaged at 0 and 24 h using an EVOS™ M7000 imaging system (Thermo Fisher Scientific, Inc; magnification, x100). ImageJ software (version 1.8.0; National Institutes of Health) was used to quantify the area occupied by cells migrating into the linear scratches.

Transwell assay. The invasion ability of the cells was assessed using the Transwell assay. In brief, Hep3B2.1-7 cells (density, $5x10^4$ cells) were suspended in plasma-free DMEM. The upper chamber was precoated with Matrigel (MilliporeSigma) and was subsequently inoculated with Hep3B2.1-7 cells (0.1 ml cell suspension/well). The lower compartment was filled with DMEM containing 20% FBS. After 24 h of incubation, the upper chamber was collected and cleaned and the cells were stained with 0.3% crystal violet (MilliporeSigma) at room temperature for 20 min. Images of cell invasion were observed under an EVOS™ M7000 imaging system (Thermo Fisher Scientific, Inc; magnification, x100).

Western blot analysis. Cells from each group were collected and the total protein was extracted using RIPA lysis buffer (Beijing Solarbio Science & Technology Co., Ltd.). Protein concentrations were determined using the BCA Protein Detection Kit (Beyotime Institute of Biotechnology) according to the manufacturer's protocol (18). The amount of total protein loaded for each group was 40 μg, which was separated by 10% SDS-PAGE and transferred to PVDF membranes (MilliporeSigma). Membranes were blocked in 5% non-fat milk (Phygene Scientific) at room temperature for 4 h. After washing for 3 times with 1X Tris-buffered saline for 5 min each, the membranes were incubated with the following primary antibodies (all purchased from Abcam) were overnight

at 4˚C: Anti-Bcl-2 (1:1,000 dilution; cat. no. Ab32124), anti-Bax (1:1,000 dilution; cat. no. Ab32503), anti-E-cadherin (1:10,000 dilution; cat. no. Ab40772), anti-N-cadherin (1:5,000 dilution; cat. no. Ab76011), anti-vimentin (1:1,000 dilution; cat. no. Ab92547), anti-CYP2J2 (1:1,000 dilution; cat. no. Ab151996) and anti-GAPDH (1:1,000 dilution; cat. no. Ab8245). Following the primary incubation, the membranes were incubated with HRP-conjugated secondary antibodies (1:5,000 dilution; Santa Cruz Biotechnology, Inc.) at room temperature for 2 h. Protein bands were visualized using ECL solution (Absin) and were imaged using a gel imager (C150; Azure Biosystems, Inc.). The gray value of the protein bands was analyzed using ImageJ (version 1.51; National Institutes of Health) with GAPDH as the loading control.

Terminal deoxynucleotidyl transferase deoxyuridine triphosphate nick-end labeling (TUNEL) assay. The effects of artemether on apoptosis of Hep3B2.1-7 cells were detected by TUNEL staining in accordance with the manufacturer's protocol. In brief, cells ($1x10^5$ cells/well) were collected and washed three times with PBS for 2 min each. Following fixing with 4% paraformaldehyde at room temperature for 5 min, the cells were gently washed with PBS twice for 2 min each time. A DAPI staining solution (cat. no. C1005; Beyotime Institute of Biotechnology) was added to just cover the cells and they were incubated at room temperature for 3-5 min. Following washing with PBS 2-3 times for 3-5 min each time, the cells were incubated with 0.3% Triton-X-100 at room temperature for 5 min. Subsequently, 50 μl TUNEL assay solution (cat. no. C1086; Beyotime Institute of Biotechnology) was added to the cells, followed by incubation at 37˚C in the dark for 60 min. The detection solution was discarded and cells were washed three times with PBS. Subsequently, three fields of view were selected at random and cells were sealed with Antifade Mounting Medium (Beyotime Institute of Biotechnology) for observation under a fluorescence microscope (magnification, x200; Zeiss GmbH).

Reverse transcription-quantitative PCR (RT-qPCR). Total RNA was isolated from cells using TRIzol® reagent according to the manufacturer's protocol. The RNA concentration and quality were assessed using a NanoDrop spectrophotometer (Thermo Fisher Scientific, Inc.). Following addition of 10 U/μl DNase I digestion solution (Roche) for 10 min at 37˚C, total RNA was reverse-transcribed into complementary DNA (cDNA) using a cDNA Synthesis Kit (Invitrogen; Thermo Fisher Scientific, Inc.). qPCR was performed using SYBR Premix Ex Taq reagents (Takara Bio, Inc.) with an ABI 7500 qPCR instrument (Applied Biosystems; Thermo Fisher Scientific, Inc.) according to the manufacturer's protocol. The following thermocycling conditions were used for qPCR: 95˚C for 10 min; followed by 40 cycles of 95˚C for 10 sec and 60˚C for 60 sec. The following primers (GenScript) were used for qPCR: CYP2J2 forward, 5'-GCCACCCCTGACACATTCAA-3' and reverse, 5'-GGCATGCCCGCTTTCCTATT-3'; and GAPDH forward, 5'-AGCCACATCGCTCAGACAC-3' and reverse, 5'-GCCCAATACGACCAAATCC-3'. GAPDH served as the internal reference gene and relative gene expression was determined using the $2^{-\Delta\Delta Cq}$ method (19).

Cell transfection. The CYP2J2-overexpression vector [overexpressed (Ov)-CYP2J2] and the corresponding negative control (NC; Ov-NC) were synthesized by Shanghai GeneChem Co., Ltd. The cells were inoculated in 12-well plates at a density of $3x10^5$ cells/well and cultured in a 5% CO_2 incubator at 37˚C for 24 h. Following incubation, cells were transfected with the aforementioned plasmids at a concentration of 20 nM using Lipofectamine® 2000 (Invitrogen; Thermo Fisher Scientific, Inc.) according to the manufacturer's protocol. Cells in the blank control group (Control) remained untreated. Following transfection for 48 h, the protein expression levels were evaluated via RT-qPCR.

Statistical analysis. All data were analyzed using GraphPad Prism 7 software (GraphPad Software, Inc.). Values are expressed as the mean ± standard deviation from ≥3 independent experimental repeats. Significant differences between two groups were determined using an unpaired Student's t-test, whereas those among more than two groups were assessed using one-way ANOVA followed by Tukey's post-hoc test. $P<0.05$ was considered to indicate a statistically significant difference.

Results

Artemether inhibits HCC cell proliferation. The effects of different concentrations of artemether on cell viability were detected using a CCK-8 assay (Fig. 1A). The results indicated that, following incubation with cells for 24, 48 and 72 h, artemether significantly inhibited the proliferation of HCC cells in a dose- and time-dependent manner (Fig. 1B and C). When the concentration of artemether was 160 μM, the viability of Hep3B2.1-7 cells decreased to 40%. Furthermore, at the same concentration, artemether exerted no significant inhibitory effect on the proliferation of HHL-5 cells, which indicated that artemether may not be harmful to healthy cells while inhibiting the proliferation of HCC cells. In addition, as presented in Fig. 1D, the colony formation assay further confirmed that artemether had a significant inhibitory effect on HCC cell proliferation. TUNEL staining indicated that artemether promoted apoptosis of HCC cells in a concentration-dependent manner (Fig. 1E). Subsequently, the expression levels of apoptosis-related proteins (Bcl-2 and Bax) were detected via western blot analysis (Fig. 1F). The results also indicated that artemether obviously promoted apoptosis of HCC cells.

Artemether inhibits HCC cell invasion and migration. Wound-healing and Transwell assays were performed to assess the effects of artemether on the invasion and migration of Hep3B2.1-7 cells after 24 h of treatment. Compared with those in the control group, the cell migration and invasion ability were decreased by artemether in a dose-dependent manner (Fig. 2A and B). Furthermore, as epithelial-mesenchymal transition (EMT) is an important internal mechanism of tumor invasion and metastasis (20), the expression levels of the EMT-related proteins E-cadherin, N-cadherin and vimentin were detected by western blot analysis. The results presented in Fig. 2C demonstrated that, compared with the control group, E-cadherin protein expression levels increased, whereas the protein expression levels of N-cadherin and vimentin

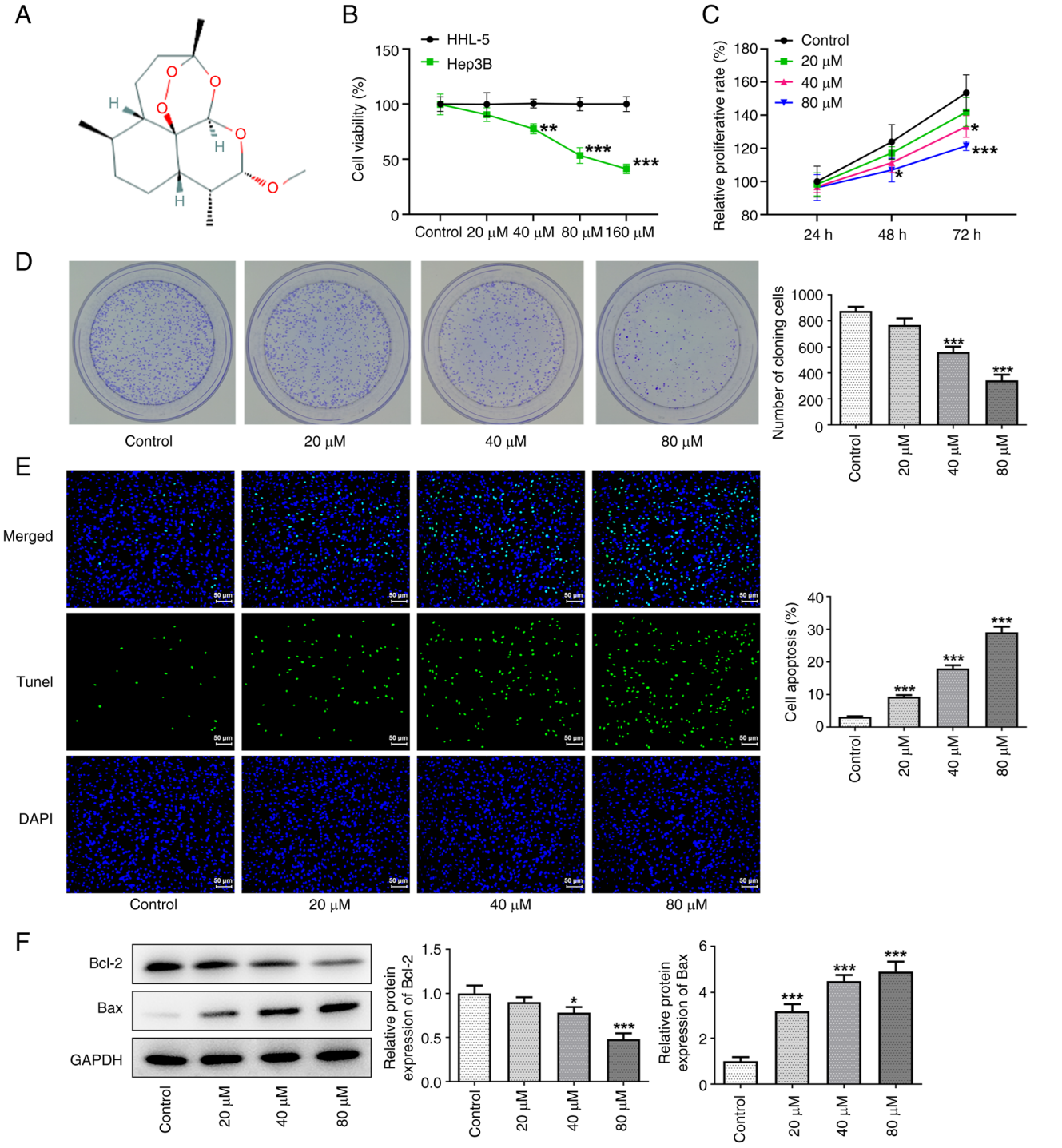

Figure 1. Artemether inhibits proliferation of hepatocellular carcinoma cells. (A) Chemical structure of artemether. (B and C) Cell proliferation was assessed by performing a Cell Counting Kit-8 assay. (B) Effects of different doses on HHL-5 and Hep3B2.1-7 cells and (C) time-dependent growth curves for Hep3B2.1-7. (D) Representative images of the colony formation assay and a diagram of its corresponding quantitative analysis. (E) TUNEL staining (scale bar, 50 μm) and (F) western blot were used to detect the effect of artemether on apoptosis of Hep 3B2.1-7 cells. *P<0.05, **P<0.01 and ***P<0.001 vs. Control. TUNEL, terminal deoxynucleotidyl transferase deoxyuridine triphosphate nick-end labeling.

decreased in a dose-dependent manner with increasing artemether concentrations. These results therefore indicated that artemether may effectively inhibit the migration and invasion of HCC cells to surrounding and distant tissues.

CYP2J2 overexpression reverses the inhibitory effect of artemether on HCC cell proliferation. It was determined that artemether may target CYP2J2 based on a prediction made with the STITCH database (Fig. 3A). In addition, the ENCORI website (https://starbase.sysu.edu.cn/) predicted no abnormal expression of CYP2J2 in HCC (Fig. 3B). Subsequently, CYP2J2 mRNA and protein expression levels in Hep3B2.1-7 cells treated with artemether were detected using RT-qPCR and western blot analysis, respectively. As presented in Fig. 3C and D, the CYP2J2 mRNA and protein expression levels decreased in a dose-dependent manner with

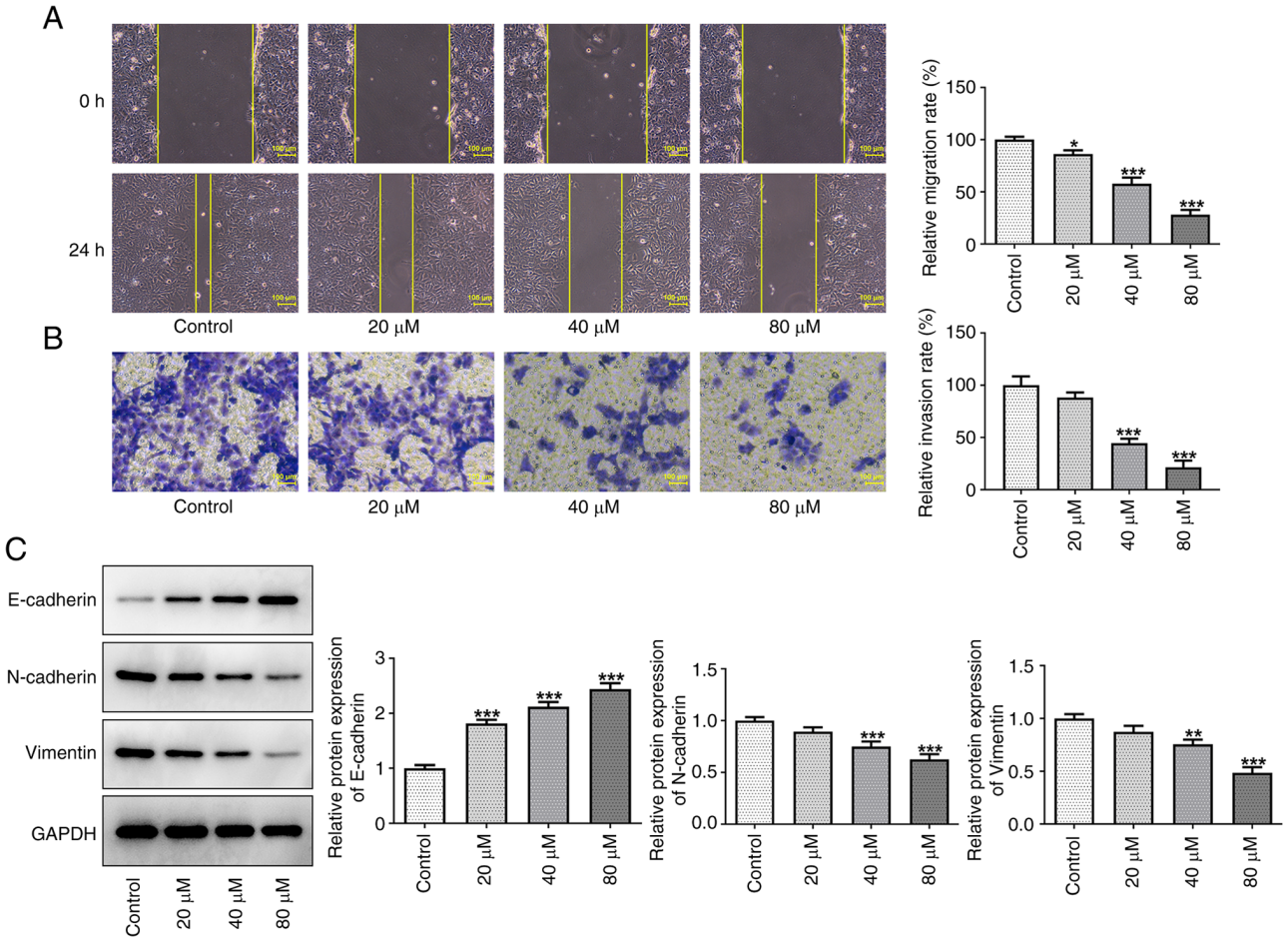

Figure 2. Artemether inhibits invasion and migration of hepatocellular carcinoma cells. (A) Representative images of the wound-healing assay (magnification, x100; scale bar, 100 μm) and quantified results. (B) Representative images of the Transwell assay (magnification, x200; scale bar, 100 μm) and quantified results. (C) E-cadherin, N-cadherin and vimentin protein expression levels were assessed by western blot analysis. *P<0.05, **P<0.01 and ***P<0.001 vs. Control.

increasing artemether concentrations. When the concentration of artemether was 80 μM, CYP2J2 mRNA and protein expression levels were at their lowest, indicating that artemether effectively inhibited CYP2J2 expression. Consequently, 80 μM artemether was selected for subsequent experiments. The transfection efficiency of the CYP2J2 overexpression plasmid in Hep3B2.1-7 cells was also detected using RT-qPCR and western blot analysis (Fig. 3E and F). The results demonstrated that the CYP2J2 mRNA and protein expression levels in the Ov-CYP2J2 group were higher compared with those in the Ov-NC group. Furthermore, CCK-8 (Fig. 3G) and colony formation assays (Fig. 3H) were applied to examine Hep3B2.1-7 cell proliferation. The results demonstrated that artemether significantly inhibited the CYP2J2 expression levels and that Ov-CYP2J2 reversed the inhibitory effect of artemether on the proliferation of HCC cells. In addition, Ov-CYP2J2 also reversed the apoptotic effect of artemether on HCC cells (Fig. 3I and J).

CYP2J2 overexpression reverses the inhibitory effect of artemether on HCC cell invasion and migration. Whether artemether affected the invasion and migration of HCC cells by targeting CYP2J2 was subsequently investigated. The results of the wound-healing and Transwell assays demonstrated that CYP2J2 overexpression significantly reversed the inhibitory effect of artemether on Hep3B2.1-7 cell invasion and migration (Fig. 4A and B). Furthermore, the elevated EMT marker E-cadherin, and the reduced N-cadherin and vimentin levels indicated that CYP2J2 overexpression counteracted the suppressive impact of artemether on the EMT process in Hep3B2.1-7 cells (Fig. 4C). These results collectively suggested that artemether may inhibit the proliferation, invasion and migration of HCC cells by targeting CYP2J2 expression.

Discussion

HCC is associated with chronic liver disease and is one of the most common and fatal cancer types worldwide (21). According to Global Cancer Statistics in 2018, HCC ranked seventh in incidence among other malignant tumors and is still the fifty-second highest cause of cancer-associated mortality worldwide (22). The mean age at diagnosis for HCC is between 50 and 60 years. Early HCC is usually treated with surgical resection, liver transplantation, ablation or radiotherapy. However, the 5-year overall survival rate following diagnosis is only 50-70% (23). Despite decades of research on cytotoxicity, targeted drugs and immunotherapy, only a limited number of effective treatment options are available for advanced HCC (24). Therefore, the development of novel therapeutics is of great significance for improving the prognosis of patients

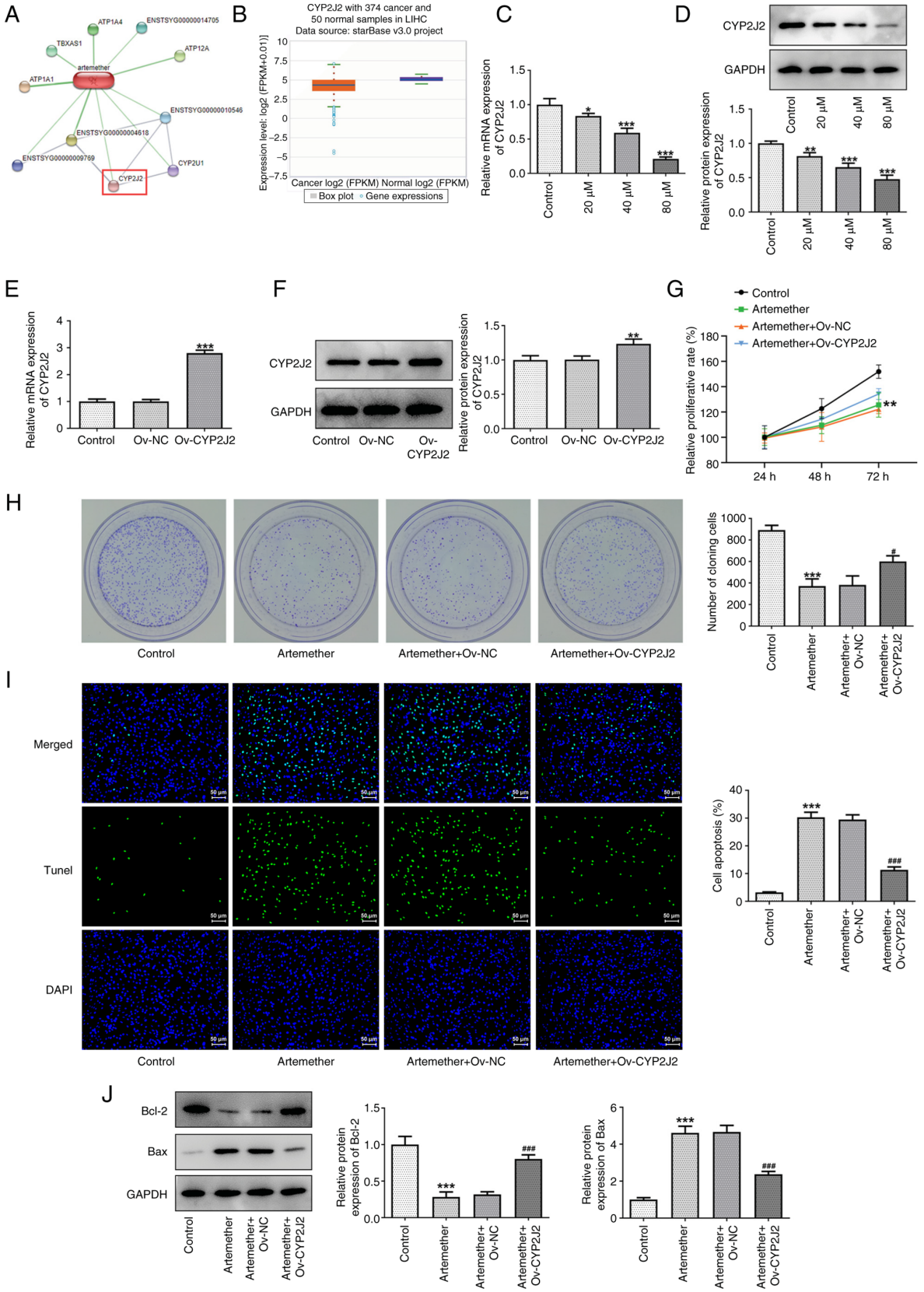

Figure 3. Overexpression of CYP2J2 reverses the inhibitory effect of artemether on the proliferation of HCC cells. (A) The artemether target CYP2J2 was analyzed using the STITCH database. (B) The ENCORI website was used to predict the expression of CYP2J2 in HCC and non-cancerous hepatocytes. (C) CYP2J2 expression levels in Hep3B2.1-7 cells were determined via reverse transcription-quantitative PCR. (D) CYP2J2 protein expression levels in Hep3B2.1-7 cells were quantified via western blot analysis. (E) CYP2J2 mRNA and (F) protein expression levels following CYP2J2 overexpression in Hep3B2.1-7 cells. (G) Cell proliferation was assessed by performing Cell Counting Kit-8 assays. (H) Representative image of the colony-formation assay and quantitative analysis of colony formation. (I) TUNEL staining (scale bar, 50 μm) and (J) western blot were used to detect the effects of Ov-CYP2J2 on apoptosis of Hep3B2.1-7 cells induced by artemether. *P<0.05, **P<0.01 and ***P<0.001 vs. Control; $^{\#}$P<0.05 and $^{\#\#\#}$P<0.001 vs. Artemether + Ov-NC. TUNEL, terminal deoxynucleotidyl transferase deoxyuridine triphosphate nick-end labeling; NC, negative control; Ov, overexpression vector; CYP2J2, cytochrome P450 family 2 subfamily J member 2; HCC, hepatocellular carcinoma.

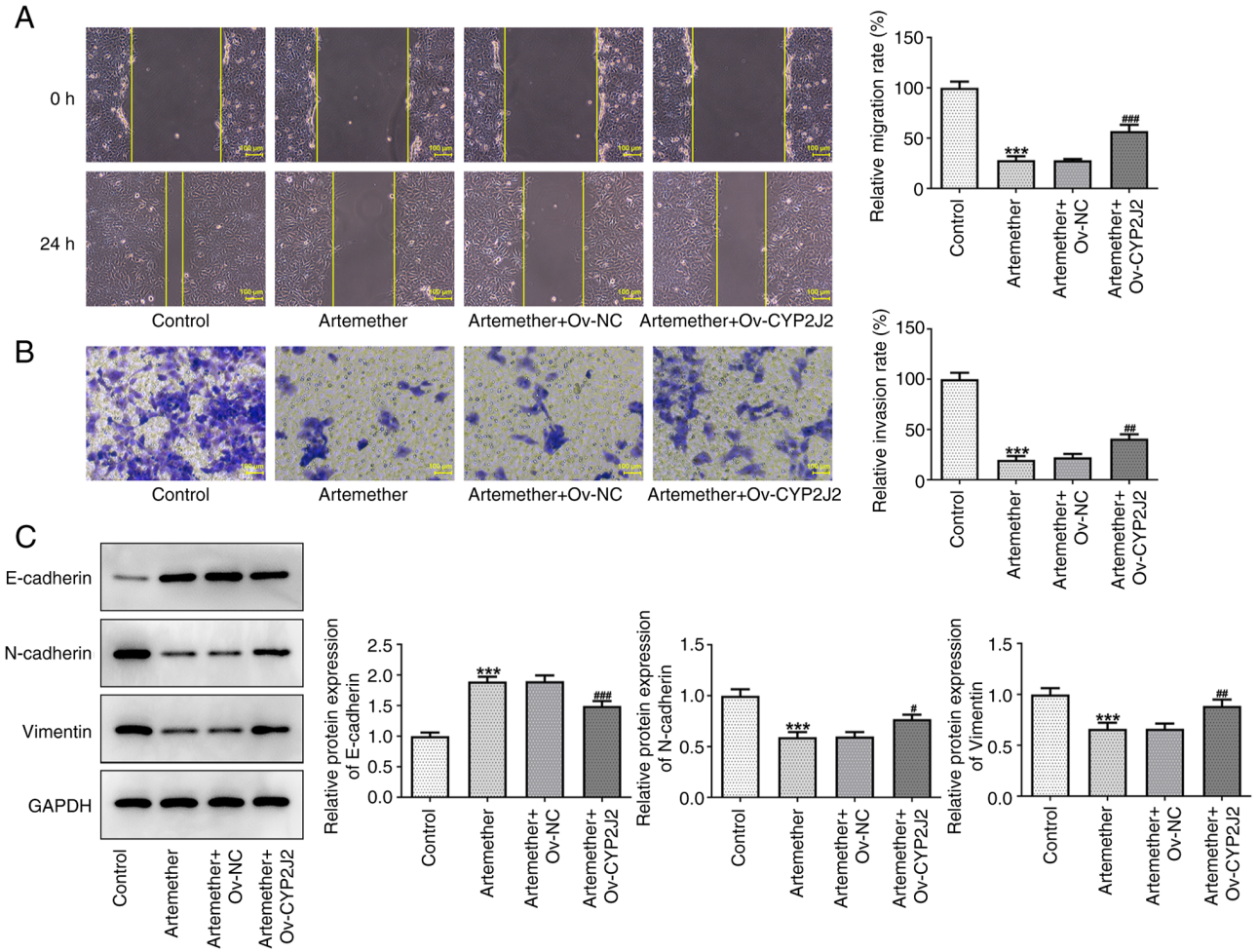

Figure 4. Overexpression of CYP2J2 reverses the inhibitory effect of artemether on the invasion and migration of hepatocellular carcinoma cells. (A) Representative images of the wound-healing assay (magnification, x100; scale bar, 100 μm) and quantified results. (B) Representative images of the Transwell assay (magnification, x200; scale bar, 100 μm) and quantified results. (C) E-cadherin, N-cadherin and vimentin protein expression levels were assessed by western blot analysis. ***P<0.001 vs. Control; $^{\#}$P<0.05, $^{\#\#}$P<0.01 and $^{\#\#\#}$P<0.001 vs. Artemether + Ov-NC. NC, negative control; Ov, overexpression vector; CYP2J2, cytochrome P450 family 2 subfamily J member 2; HCC, hepatocellular carcinoma.

with HCC. In the present study, the results demonstrated that artemether inhibited the proliferation and induced apoptosis of Hep3B2.1-7 cells in a dose-dependent manner, which may be related to the ability of artemether to induce cell cycle arrest/growth inhibition (25). This is consistent with the results of the study by Hou *et al* (25), which examined the effect of artemisinin on the cell cycle of liver cancer cells, indicating that after artemisinin treatment of HepG2 cells, the proportion of cells in G1 phase was significantly increased, with higher concentrations inducing more significant G1-phase arrest.

Artemisinin and its derivatives have long been recognized as the most effective anti-malarial drugs worldwide (2,26,27). With the further development of artemisinin and its derivatives, studies have reported that they possess good antitumor activity in the treatment of human cancer (28-30). Artemether, as a natural derivative of artemisinin, may also be more effective than artemisinin (31). It was demonstrated that when using artemether and triglyceride docosahexaenoate as a lipid core, nanoemulsion, nanostructure lipid carrier and poly (lactic acid)-poly (ethylene glycol), nanocapsules were successfully prepared to reduce the activity, proliferation and migration of MDA-MB-231 and MCF-7 breast cancer cells in a dose-dependent manner (32). Furthermore, artemether was able to regulate the sensitivity of B7-H3 human neuroblastoma cells to adriamycin (33). Interference with vascular cell adhesion protein-1 in combination with short hairpin-RNA significantly inhibited the malignant behavior of human glioma cells (34). These properties make artemether an attractive potential candidate for chemotherapy. However, to the best of our knowledge, the efficacy of artemether in HCC has remained elusive. In the present study, artemether significantly reduced the activity of Hep3B2.1-7 cells and promoted apoptosis in a dose-dependent manner. These results verified the antitumor effect of artemether in HCC.

To further explore the mechanism of artemether in HCC, the STITCH database was used to predict that artemether is able to target CYP2J2. As previously mentioned, CYP2J2 is a cyclooxygenase that is able to metabolize numerous unsaturated fatty acids and serves a variety of biological roles in the cardiovascular system and a number of solid human cancer types (12,35,36). For instance, Park *et al* (37) demonstrated that CYPs inhibit the proliferation of human HCC cells and lead to apoptosis via non-competitive inhibition of the CYP2J2 enzyme. Furthermore, Allison *et al* (38) demonstrated that

paclitaxel, a chemotherapeutic drug, induces apoptosis in breast cancer cells via mediating lipid peroxidation and generating reactive oxygen species, but CYP2J2 overexpression was able to activate aldehyde dehydrogenase 1 family member A1, which reversed the inhibitory effect of paclitaxel on tumor growth. Another study also reported that acetylshikonin exerted inhibitory effects against CYP2J2 and anti-cancer activity in human liver cancer HepG2 cells (37). In the present study, it was confirmed that artemether inhibited the expression of CYP2J2 in a concentration-dependent manner and further overexpression of CYP2J2 revealed that Ov-CYP2J2 partially reversed the inhibitory effects of artemether on the proliferation, migration and invasion of HCC cells.

The present study had several limitations. First, the mechanism of the effect of artemether on Hep3B2.1-7 cells was assessed by overexpression of CYP2J2. However, other methods, such as CYP2J2 antagonists or inhibitors, may be useful to confirm the present observations. Furthermore, *in vitro* studies using only Hep3B2.1-7 cells were performed in the present study and other HCC cell lines or animal experiments may provide additional information to complement the current findings. In addition, further evaluation of the effect of artemether on the cell cycle of HCC cells and verification of the upregulation of CYP2J2 expression in HCC compared with normal hepatocytes will be endeavored in a future study.

In conclusion, artemether inhibited the activity of Hep3B2.1-7 cells in a dose-dependent manner. The results of the present study suggested that artemether suppressed the proliferation and activity of HCC by targeting CYP2J2. Therefore, the development of effective CYP2J2 inhibitors may be of potential therapeutic value. In future work, the specific anticancer mechanism of artemether will continue to be investigated and *in vivo* experiments in mice will also be performed.

Acknowledgements

Not applicable.

Funding

No funding was received.

Availability of data and materials

The datasets used and/or analyzed during the current study are available from the corresponding author on reasonable request.

Authors' contributions

XZ and MY conceptualized and designed the current study. GY, ZS and QS acquired, analyzed and interpreted data. QS, XZ and MY drafted the manuscript and revised it critically for important intellectual content. All authors agreed to be held accountable for the current study in ensuring questions related to the integrity of any part of the work are appropriately investigated and resolved. XZ and QS confirm the authenticity of the raw data. All authors read approved the final manuscript.

Ethics approval and consent to participate

Not applicable.

Patient consent for publication

Not applicable.

Competing interests

The authors declare that they have no competing interests.

References

1. Esu EB, Effa EE, Opie ON and Meremikwu MM: Artemether for severe malaria. Cochrane Database Syst Rev 6: CD010678, 2019.
2. Visser BJ, Bierhoff M, van Gool T, van Hattem JM, Grobusch MP and van Vugt M: The treatment of malaria. Ned Tijdschr Geneeskd 163: D3321, 2019 (In Dutch).
3. Cheong DHJ, Tan DWS, Wong FWS and Tran T: Anti-malarial drug, artemisinin and its derivatives for the treatment of respiratory diseases. Pharmacol Res 158: 104901, 2020.
4. Prabhu P, Suryavanshi S, Pathak S, Patra A, Sharma S and Patravale V: Nanostructured lipid carriers of artemether-lumefantrine combination for intravenous therapy of cerebral malaria. Int J Pharm 513: 504-517, 2016.
5. Ouji M, Barnoin G, Fernandez Alvarez A, Augereau JM, Hemmert C, Benoit-Vical F and Gornitzka H: Hybrid Gold(I) NHC-artemether complexes to target falciparum malaria parasites. Molecules 25: 2817, 2020.
6. Chen J, Huang X, Tao C, Xiao T, Li X, Zeng Q, Ma M and Wu Z: Artemether attenuates the progression of non-small cell lung cancer by inducing apoptosis, cell cycle arrest and promoting cellular senescence. Biol Pharm Bull 42: 1720-1725, 2019.
7. Wu J, Li L, Wang Y, Ren X, Lin K and He Y: The HSP90/Akt pathway may mediate artemether-induced apoptosis of Cal27 cells. FEBS Open Bio 9: 1726-1733, 2019.
8. Zhao X, Guo X, Yue W, Wang J, Yang J and Chen J: Artemether suppresses cell proliferation and induces apoptosis in diffuse large B cell lymphoma cells. Exp Ther Med 14: 4083-4090, 2017.
9. Robinson JF, Hamilton EG, Lam J, Chen H and Woodruff TJ: Differences in cytochrome p450 enzyme expression and activity in fetal and adult tissues. Placenta 100: 35-44, 2020.
10. Lee CM, Lee J, Jang SN, Shon JC, Wu Z, Park K, Liu KH and Park SH: 6,8-diprenylorobol induces apoptosis in human hepatocellular carcinoma cells via activation of FOXO3 and inhibition of CYP2J2. Oxid Med Cell Longev 2020: 8887251, 2020.
11. Zou X and Mo Z: CYP2J2 is a diagnostic and prognostic biomarker associated with immune infiltration in kidney renal clear cell carcinoma. Biomed Res Int 2021: 3771866, 2021.
12. Evangelista EA, Aliwarga T, Sotoodehnia N, Jensen PN, McKnight B, Lemaitre RN, Totah RA and Gharib SA: CYP2J2 modulates diverse transcriptional programs in adult human cardiomyocytes. Sci Rep 10: 5329, 2020.
13. Bièche I, Narjoz C, Asselah T, Vacher S, Marcellin P, Lidereau R, Beaune P and de Waziers I: Reverse transcriptase-PCR quantification of mRNA levels from cytochrome (CYP)1, CYP2 and CYP3 families in 22 different human tissues. Pharmacogenet Genomics 17: 731-742, 2007.
14. Tao P, Jiang Y, Wang H and Gao G: CYP2J2-produced epoxyeicosatrienoic acids contribute to the ferroptosis resistance of pancreatic ductal adenocarcinoma in a PPARγ-dependent manner. Zhong Nan Da Xue Xue Bao Yi Xue Ban 46: 932-941, 2021 (In Chinese).
15. Jiang JG, Chen CL, Card JW, Yang S, Chen JX, Fu XN, Ning YG, Xiao X, Zeldin DC and Wang DW: Cytochrome P450 2J2 promotes the neoplastic phenotype of carcinoma cells and is up-regulated in human tumors. Cancer Res 65: 4707-4715, 2005.
16. Lei X, Chen X, Quan Y, Tao Y and Li J: Targeting CYP2J2 to enhance the anti-glioma efficacy of cannabinoid receptor 2 stimulation by inhibiting the pro-angiogenesis function of M2 microglia. Front Oncol 10: 574277, 2020.
17. Gui L, Xu Q, Huang J, Wu G, Tang H, Hui L, Hua P, Zhang L and Zhu Y: CYP2J2 promotes the development of hepatocellular carcinoma by increasing the EETs production to improve HIF-1α stability. Am J Transl Res 12: 7923-7937, 2020.

18. Khramtsov P, Kalashnikova T, Bochkova M, Kropaneva M, Timganova V, Zamorina S and Rayev M: Measuring the concentration of protein nanoparticles synthesized by desolvation method: Comparison of Bradford assay, BCA assay, hydrolysis/UV spectroscopy and gravimetric analysis. Int J Pharm 599: 120422, 2021.
19. Hirschfeld M, Ge I, Rucker G, Waldschmidt J, Mayer S, Jager M, Voigt M, Kammerer B, Nöthling C, Berner K, *et al*: Mutually distinguishing microRNA signatures of breast, ovarian and endometrial cancers in vitro. Mol Med Rep 22: 4048-4060, 2020.
20. Zhang Y and Weinberg RA: Epithelial-to-mesenchymal transition in cancer: Complexity and opportunities. Front Med 12: 361-373, 2018.
21. Hartke J, Johnson M and Ghabril M: The diagnosis and treatment of hepatocellular carcinoma. Semin Diagn Pathol 34: 153-159, 2017.
22. Bray F, Ferlay J, Soerjomataram I, Siegel RL, Torre LA and Jemal A: Global cancer statistics 2018: GLOBOCAN estimates of incidence and mortality worldwide for 36 cancers in 185 countries. CA Cancer J Clin 68: 394-424, 2018.
23. European Association for the Study of the Liver. Electronic address: Easloffice@easloffice.eu; European Association for the Study of the Liver: 'EASL Clinical Practice Guidelines: Management of hepatocellular carcinoma' J Hepatol 69: 182-236, 2018.
24. An Y, Jiang J, Zhou L, Shi J, Jin P, Li L, Peng L, He S, Zhang W, Huang H, *et al*: Peroxiredoxin 1 is essential for natamycin-triggered apoptosis and protective autophagy in hepatocellular carcinoma. Cancer Lett 521: 210-223, 2021.
25. Hou J, Wang D, Zhang R and Wang H: Experimental therapy of hepatoma with artemisinin and its derivatives: In vitro and in vivo activity, chemosensitization, and mechanisms of action. Clin Cancer Res 14: 5519-5530, 2008.
26. Talman AM, Clain J, Duval R, Menard R and Ariey F: Artemisinin bioactivity and resistance in malaria parasites. Trends Parasitol 35: 953-963, 2019.
27. Menard D and Dondorp A: Antimalarial drug resistance: A threat to malaria elimination. Cold Spring Harb Perspect Med 7: a025619, 2017.
28. Cao Y, Feng YH, Gao LW, Li XY, Jin QX, Wang YY, Xu YY, Jin F, Lu SL and Wei MJ: Artemisinin enhances the anti-tumor immune response in 4T1 breast cancer cells in vitro and in vivo. Int Immunopharmacol 70: 110-116, 2019.
29. Jiang F, Zhou JY, Zhang D, Liu MH and Chen YG: Artesunate induces apoptosis and autophagy in HCT116 colon cancer cells, and autophagy inhibition enhances the artesunate-induced apoptosis. Int J Mol Med 42: 1295-1304, 2018.
30. Zhao F, Vakhrusheva O, Markowitsch SD, Slade KS, Tsaur I, Cinatl J Jr, Michaelis M, Efferth T, Haferkamp A and Juengel E: Artesunate impairs growth in cisplatin-resistant bladder cancer cells by cell cycle arrest, apoptosis and autophagy induction. Cells 9: 2643, 2020.
31. Zhang Y, Xu G, Zhang S, Wang D, Saravana Prabha P and Zuo Z: Antitumor research on artemisinin and its bioactive derivatives. Nat Prod Bioprospect 8: 303-319, 2018.
32. Lanna EG, Siqueira RP, Machado MGC, de Souza A, Trindade IC, Branquinho RT and Mosqueira VCF: Lipid-based nanocarriers co-loaded with artemether and triglycerides of docosahexaenoic acid: Effects on human breast cancer cells. Biomed Pharmacother 134: 111114, 2021.
33. Tan WQ, Chen G, Ye M and Jia B: Artemether regulates chemosensitivity to doxorubicin via regulation of B7-H3 in human neuroblastoma cells. Med Sci Monit 23: 4252-4259, 2017.
34. Wang YB, Hu Y, Li Z, Wang P, Xue YX, Yao YL, Yu B and Liu YH: Artemether combined with shRNA interference of vascular cell adhesion molecule-1 significantly inhibited the malignant biological behavior of human glioma cells. PLoS One 8: e60834, 2013.
35. Aliwarga T, Evangelista EA, Sotoodehnia N, Lemaitre RN and Totah RA: Regulation of CYP2J2 and EET levels in cardiac disease and diabetes. Int J Mol Sci 19: 1916, 2018.
36. Das A, Weigle AT, Arnold WR, Kim JS, Carnevale LN and Huff HC: CYP2J2 molecular recognition: A new axis for therapeutic design. Pharmacol Ther 215: 107601, 2020.
37. Park SH, Phuc NM, Lee J, Wu Z, Kim J, Kim H, Kim ND, Lee T, Song KS and Liu KH: Identification of acetylshikonin as the novel CYP2J2 inhibitor with anti-cancer activity in HepG2 cells. Phytomedicine 24: 134-140, 2017.
38. Allison SE, Chen Y, Petrovic N, Zhang J, Bourget K, Mackenzie PI and Murray M: Activation of ALDH1A1 in MDA-MB-468 breast cancer cells that over-express CYP2J2 protects against paclitaxel-dependent cell death mediated by reactive oxygen species. Biochem Pharmacol 143: 79-89, 2017.